TABLE 4 (Continued)

	English		Japanese			English		Japanese	
4	22	2.51	3	0.82	4	84	9.59	29	7.95
999	7	0.8	0	0.00	999	10	1.14	1	0.27
Total	876	100	365	100.00	Total	876	100	365	100.00
Saliva and drooling*	Frequency	%	Frequency	%	Turning in bed	Frequency	%	Frequency	%
0	341	38.93	186	50.96	0	277	31.62	122	33.42
1	115	13.13	49	13.42	1	378	43.15	144	39.45
2	203	23.17	64	17.53	2	111	12.67	48	13.15
3	157	17.92	46	12.60	3	55	6.28	31	8.49
4	53	6.05	18	4.93	4	50	5.71	19	5.21
999	7	0.8	2	0.55	999	5	0.57	1	0.27
Total	876	100	365	100.00	Total	876	100	365	100.00
Chewing and swallowing	Frequency	%	Frequency	%	Tremor*	Frequency	%	Frequency	%
0	549	62.67	241	66.03	0	189	21.58	118	32.33
1	230	26.26	81	22.19	1	360	41.1	154	42.19
2	54	6.16	22	6.03	2	212	24.2	69	18.90
3	34	3.88	18	4.93	3	72	8.22	17	4.66
4	3	0.34	3	0.82	4	36	4.11	7	1.92
999	6	0.68	0	0.00	999	7	0.8	0	0.00
Total	876	100	365	100.00	Total	876	100	365	100.00
Eating tasks	Frequency	%	Frequency	%	Getting out of bed*	Frequency	%	Frequency	%
0	363	41.44	158	43.29	0	180	**20.55**	**101**	27.67
1	265	30.25	114	31.23	1	317	36.19	140	38.36
2	187	21.35	79	21.64	2	199	22.72	73	20.00
3	42	4.79	8	2.19	3	104	11.87	35	9.59
4	10	1.14	5	1.37	4	70	7.99	15	4.11
999	9	1.03	1	0.27	999	6	0.68	1	0.27
Total	876	100	365	100.00	Total	876	100	365	100.00
Dressing	Frequency	%	Frequency	%	Walking and balance	Frequency	%	Frequency	%
0	220	25.11	82	22.47	0	184	21	74	20.27
1	322	36.76	176	48.22	1	336	38.36	156	42.74
2	211	24.09	67	18.36	2	105	11.99	38	10.41
3	76	8.68	28	7.67	3	172	19.63	61	16.71
4	42	4.79	12	3.29	4	74	8.45	33	9.04
999	5	0.57	0	0.00	999	5	0.57	3	0.82
Total	876	100	365	100.00	Total	876	100	365	100.00
Hygiene	Frequency	%	Frequency	%	Freezing	Frequency	%	Frequency	%
0	342	39.04	126	34.52	0	453	51.71	176	48.22
1	367	41.89	160	43.84	1	182	20.78	74	20.27
2	88	10.05	47	12.88	2	89	10.16	40	10.96
3	33	3.77	25	6.85	3	90	10.27	49	13.42
4	38	4.34	7	1.92	4	56	6.39	25	6.85
999	8	0.91	0	0.00	999	6	0.68	1	0.27
Total	876	100	365	100.00	Total	876	100	365	100.00
Handwriting	Frequency	%	Frequency	%					
0	161	18.38	106	29.04					
1	251	28.65	151	41.37					
2	222	25.34	75	20.55					
3	146	16.67	22	6.03					
Part III									
Speech*	Frequency	%	Frequency	%	Arising from chair	Frequency	%	Frequency	%
0	189	21.58	148	40.55	0	422	48.17	197	53.97
1	379	43.26	143	39.18	1	245	27.97	106	29.04
2	213	24.32	53	14.52	2	78	8.9	24	6.58
3	69	7.88	15	4.11	3	71	8.11	22	6.03
4	22	2.51	4	1.10	4	55	6.28	16	4.38
999	4	0.46	2	0.55	999	5	0.57	0	0.00
Total	876	100	365	100.00	Total	876	100	365	100.00
Facial expression*	Frequency	%	Frequency	%	Gait	Frequency	%	Frequency	%
0	96	10.96	88	24.11	0	202	23.06	81	22.19
1	300	34.25	137	37.53	1	351	40.07	187	51.23
2	361	41.21	109	29.86	2	167	19.06	47	12.88
3	89	10.16	23	6.30	3	97	11.07	36	9.86
4	26	2.97	7	1.92	4	55	6.28	14	3.84
999	4	0.46	1	0.27	999	4	0.46	0	0.00
Total	876	100	365	100.00	Total	876	100	365	100.00
Rigidity, neck	Frequency	%	Frequency	%	Freezing of gait	Frequency	%	Frequency	%
0	260	29.68	134	36.71	0	655	74.77	250	68.49
1	247	28.2	97	26.58	1	95	10.84	50	13.70
2	274	31.28	92	25.21	2	60	6.85	30	8.22
3	73	8.33	36	9.86	3	26	2.97	13	3.56

doi:10.1002/mdc3.12058

TABLE 4 (Continued)

	English		Japanese			English		Japanese	
4	16	1.83	4	1.10	4	38	4.34	19	5.21
999	6	0.68	2	0.55	999	2	0.23	3	0.82
Total	876	100	365	100.00	Total	876	100	365	100.00
Rigidity, RUE*	Frequency	%	Frequency	%	Postural stability*	Frequency	%	Frequency	%
0	176	20.09	93	25.48	0	422	48.17	150	41.10
1	282	32.19	142	38.90	1	157	17.92	66	18.08
2	342	39.04	111	30.41	2	60	6.85	44	12.05
3	69	7.88	14	3.84	3	149	17.01	84	23.01
4	6	0.68	2	0.55	4	86	9.82	20	5.48
999	1	0.11	3	0.82	999	2	0.23	1	0.27
Total	876	100	365	100.00	Total	876	100	365	100.00
Rigidity, LUE*	Frequency	%	Frequency	%	Posture	Frequency	%	Frequency	%
0	205	23.4	99	27.12	0	173	19.75	78	21.37
1	268	30.59	135	36.99	1	337	38.47	129	35.34
2	317	36.19	121	33.15	2	206	23.52	84	23.01
3	77	8.79	9	2.47	3	125	14.27	52	14.25
4	7	0.8	1	0.27	4	33	3.77	21	5.75
999	2	0.23	0	0.00	999	2	0.23	1	0.27
Total	876	100	365	100.00	Total	876	100	365	100.00
Rigidity, RLE	Frequency	%	Frequency	%	Global spontaneity of movement	Frequency	%	Frequency	%
0	272	31.05	109	29.86	0	108	12.33	49	13.42
1	248	28.31	125	34.25	1	278	31.74	155	42.47
2	275	31.39	106	29.04	2	279	31.85	97	26.58
3	67	7.65	23	6.30	3	184	21	51	13.97
4	10	1.14	1	0.27	4	27	3.08	12	3.29
999	4	0.46	1	0.27	999	0	0	1	0.27
Total	876	100	365	100.00	Total	876	100	365	100.00
Rigidity, LLE	Frequency	%	Frequency	%	Postural tremor, right hand	Frequency	%	Frequency	%
0	286	32.65	116	31.78	0	544	62.1	223	61.10
1	227	25.91	120	32.88	1	262	29.91	119	32.60
2	275	31.39	100	27.40	2	43	4.91	19	5.21
3	75	8.56	26	7.12	3	23	2.63	2	0.55
4	11	1.26	1	0.27	4	1	0.11	2	0.55
999	2	0.23	2	0.55	999	3	0.34	0	0.00
Total	876	100	365	100.00	Total	876	100	365	100.00
Finger tapping, right hand*	Frequency	%	Frequency	%	Postural tremor, left hand*	Frequency	%	Frequency	%
0	122	13.93	95	26.03	0	518	59.13	234	64.11
1	342	39.04	167	45.75	1	276	31.51	98	26.85
2	252	28.77	64	17.53	2	49	5.59	27	7.40
3	144	16.44	35	9.59	3	29	3.31	2	0.55
4	15	1.71	3	0.82	4	1	0.11	1	0.27
999	1	0.11	1	0.27	999	3	0.34	3	0.82
Total	876	100	365	100.00	Total	876	100	365	100.00
Finger tapping, left hand*	Frequency	%	Frequency	%	Kinetic tremor, right hand*	Frequency	%	Frequency	%
0	108	12.33	91	24.93	0	546	62.33	258	70.68
1	298	34.02	135	36.99	1	265	30.25	89	24.38
2	265	30.25	96	26.30	2	46	5.25	15	4.11
3	181	20.66	37	10.14	3	13	1.48	1	0.27
4	22	2.51	5	1.37	4	2	0.23	1	0.27
999	2	0.23	1	0.27	999	4	0.46	1	0.27
Total	876	100	365	100.00	Total	876	100	365	100.00
Hand movements, right hand*	Frequency	%	Frequency	%	Kinetic tremor, left hand*	Frequency	%	Frequency	%
0	187	21.35	129	35.34	0	493	56.28	236	64.66
1	346	39.5	160	43.84	1	293	33.45	105	28.77
2	231	26.37	57	15.62	2	72	8.22	22	6.03
3	98	11.19	17	4.66	3	14	1.6	1	0.27
4	12	1.37	2	0.55	4	0	0	1	0.27
999	2	0.23	0	0.00	999	4	0.46	0	0.00
Total	876	100	365	100.00	Total	876	100	365	100.00
Hand movements, left hand*	Frequency	%	Frequency	%	Rest tremor amplitude, RUE*	Frequency	%	Frequency	%
0	164	18.72	118	32.33	0	586	66.89	281	76.99
1	311	35.5	147	40.27	1	112	12.79	51	13.97
2	250	28.54	78	21.37	2	121	13.81	26	7.12
3	125	14.27	17	4.66	3	53	6.05	6	1.64

doi:10.1002/mdc3.12058

TABLE 4 (Continued)

	English		Japanese			English		Japanese	
4	25	2.85	4	1.10	4	3	0.34	1	0.27
999	1	0.11	1	0.27	999	1	0.11	0	0.00
Total	876	100	365	100.00	Total	876	100	365	100.00
Pronation: supination movements, right hand*	Frequency	%	Frequency	%	Rest tremor amplitude, LUE*	Frequency	%	Frequency	%
0	199	22.72	100	27.40	0	603	68.84	280	76.71
1	335	38.24	159	43.56	1	120	13.7	56	15.34
2	216	24.66	64	17.53	2	99	11.3	20	5.48
3	107	12.21	35	9.59	3	45	5.14	9	2.47
4	17	1.94	6	1.64	4	5	0.57	0	0.00
999	2	0.23	1	0.27	999	4	0.46	0	0.00
Total	876	100	365	100.00	Total	876	100	365	100.00
Pronation: supination movements, left hand	Frequency	%	Frequency	%	Rest tremor amplitude, RLE	Frequency	%	Frequency	%
0	162	18.49	76	20.82	0	777	88.7	319	87.40
1	297	33.9	138	37.81	1	52	5.94	25	6.85
2	235	26.83	101	27.67	2	35	4	18	4.93
3	150	17.12	42	11.51	3	9	1.03	2	0.55
4	29	3.31	8	2.19	4	0	0	0	0.00
999	3	0.34	0	0.00	999	3	0.34	1	0.27
Total	876	100	365	100.00	Total	876	100	365	100.00
Toe tapping, right foot*	Frequency	%	Frequency	%	Rest tremor amplitude, LLE	Frequency	%	Frequency	%
0	168	19.18	89	24.38	0	795	90.75	319	87.40
1	323	36.87	149	40.82	1	46	5.25	24	6.58
2	228	26.03	96	26.30	2	20	2.28	17	4.66
3	129	14.73	24	6.58	3	12	1.37	2	0.55
4	27	3.08	6	1.64	4	0	0	0	0.00
999	1	0.11	1	0.27	999	3	0.34	3	0.82
Total	876	100	365	100.00	Total	876	100	365	100.00
Toe tapping, left foot*	Frequency	%	Frequency	%	Rest tremor amplitude, lip/jaw*	Frequency	%	Frequency	%
0	154	17.58	68	18.63	0	780	89.04	349	95.62
1	251	28.65	140	38.36	1	63	7.19	12	3.29
2	268	30.59	111	30.41	2	18	2.05	3	0.82
3	154	17.58	36	9.86	3	13	1.48	0	0.00
4	46	5.25	10	2.74	4	1	0.11	1	0.27
999	3	0.34	0	0.00	999	1	0.11	0	0.00
Total	876	100	365	100.00	Total	876	100	365	100.00
Leg agility, right leg*	Frequency	%	Frequency	%	Constancy of rest*	Frequency	%	Frequency	%
0	250	28.54	119	32.60	0	409	46.69	219	60.00
1	329	37.56	163	44.66	1	214	24.43	79	21.64
2	190	21.69	61	16.71	2	91	10.39	28	7.67
3	86	9.82	18	4.93	3	85	9.7	21	5.75
4	18	2.05	4	1.10	4	67	7.65	17	4.66
999	3	0.34	0	0.00	999	10	1.14	1	0.27
Total	876	100	365	100.00	Total	876	100	365	100.00
Leg agility, left leg*	Frequency	%	Frequency	%					
0	216	24.66	99	27.12					
1	298	34.02	142	38.90					
2	213	24.32	90	24.66					
3	106	12.1	30	8.22					
4	38	4.34	3	0.82					
999	5	0.57	1	0.27					
Total	876	100	365	100.00					
Part IV									
Time spent with dyskinesias*	Frequency	%	Frequency	%	Functional impact of fluctuations	Frequency	%	Frequency	%
0	563	64.27	273	74.79	0	433	49.43	194	53.15
1	173	19.75	41	11.23	1	165	18.84	56	15.34
2	87	9.93	30	8.22	2	81	9.25	32	8.77
3	27	3.08	12	3.29	3	119	13.58	60	16.44
4	17	1.94	6	1.64	4	63	7.19	19	5.21
999	9	1.03	3	0.82	999	15	1.71	4	1.10
Total	876	100	365	100.00	Total	876	100	365	100.00

doi:10.1002/mdc3.12058

TABLE 4 (Continued)

	English		Japanese			English		Japanese	
Functional impact of dyskinesias*	Frequency	%	Frequency	%	Complexity of motor fluctuations*	Frequency	%	Frequency	%
0	695	79.34	308	84.38	0	404	46.12	192	52.60
1	90	10.27	27	7.40	1	291	33.22	125	34.25
2	29	3.31	19	5.21	2	69	7.88	21	5.75
3	46	5.25	7	1.92	3	50	5.71	17	4.66
4	5	0.57	2	0.55	4	46	5.25	3	0.82
999	11	1.26	2	0.55	999	16	1.83	7	1.92
Total	876	100	365	100.00	Total	876	100	365	100.00
Time spent in the OFF state*	Frequency	%	Frequency	%	Painful OFF state dystonia*	Frequency	%	Frequency	%
0	383	43.72	183	50.14	0	680	77.63	319	87.40
1	341	38.93	113	30.96	1	114	13.01	28	7.67
2	106	12.1	50	13.70	2	45	5.14	4	1.10
3	22	2.51	14	3.84	3	13	1.48	6	1.64
4	14	1.6	2	0.55	4	15	1.71	5	1.37
999	10	1.14	3	0.82	999	9	1.03	3	0.82
Total	876	100	365	100.00	Total	876	100	365	100.00

[a]999 = missing.
*$P < 0.05$ by chi-square test (df = 4).
DDS, dopamine dysregulation syndrome; RUE, right upper extremity; LUE, left upper extremity; RLE, right lower extremity; LLE, left lower extremity.

Author Roles

(1) Research Project: A. Conception, B. Organization, C. Execution; (2) Statistical Analysis: A. Design, B. Execution, C. Review and Critique; (3) Manuscript: A. Writing of the First Draft, B. Review and Critique.

K. Kashihara: 1A, 1B, 1C, 2C, 3A, 3B
T. Kondo: 1A, 1B, 1C, 3A, 3B
Y. Mizuno: 1A, 1B, 1C, 3A, 3B
S. Kikuchi: 1B, 1C, 3B
S. Kuno: 1B, 1C, 3B
K. Hasegawa: 1B, 1C, 3A, 3B
N. Hattori: 1B, 1C, 3B
H. Mochizuki: 1B, 1C, 3B
H. Mori: 1B, 1C, 3B
M. Murata: 1B, 1C, 3B
M. Nomoto: 1B, 1C, 3B
R. Takahashi: 1B, 1C, 3B
A. Takeda: 1B, 1C, 3B
Y. Tsuboi: 1B, 1C, 3B
Y. Ugawa: 1B, 1C, 3B
M. Yamamoto: 1B, 1C, 3B
F. Yokochi: 1B, 1C, 3B
F. Yoshii: 1A, 1B, 1C, 3A, 3B
G.T. Stebbins: 1A, 1B, 1C, 2A, 2C, 3B
B.C. Tilley: 2C, 3B
L. Wang: 2B, 2C, 3A, 3B
S. Luo: 2C, 3B
N.R. LaPelle: 2A, 2B, 3B
C.G. Goetz: 1A, 1B, 1C, 2A, 2C, 3A, 3B

Disclosures

Funding Sources and Conflicts of Interest: This work was supported by Boehringer Ingelheim Japan. The administrative core members (G.T.S., B.C.T., S.L., L.W., N.R.L., and C.G.G.) were supported by funds from the Movement Disorder Society.

Financial Disclosures for previous 12 months: Kenichi Kashihara has served on the advisory board of Kyowa Hakko Kirin Co.; has been supported by Health and Labor Sciences Research Grants; has received honoraria from Boehringer Ingelheim, GlaxoSmithKline (GSK), Kyowa Hakko Kirin Co., Novartis, Otsuka Pharmaceutical Co., Dainippon Sumitomo Pharm Co., Ltd., and Fujimoto Pharmaceutical (FP) Pharmaceutical Co.; and has received royalties from Nankodo. Tomoyoshi Kondo has worked as a consultant for Kyowa Hakko Kirin Co. and Novartis and has received honoraria from Boeringer Ingelheim, GSK, Kyowa Hakko Kirin Co., Novartis, Otsuka Pharmaceutical Co., Dainippon Sumitomo Pharm Co., Ltd., and FP Pharmaceutical Co. Yoshikuni Mizuno has held advisory board membership with FP Pharmaceutical Co., Otsuka Pharmaceutical Co., AbbVie Japan, and Kyowa Hakko Kirin Co. and received personal compensation when he attended advisory board meetings and has been supported by grants from Boehringer Ingelheim. Seiji Kikuchi has been supported by grants from the Ministry of Health, Labor and Welfare of Japan and has received honoraria from Boehringer Ingelheim, GSK, Kyowa Hakko Kirin Co., Novartis, Otsuka Pharmaceutical Co., Dainippon Sumitomo Pharm Co., Ltd., FP Pharmaceutical Co., Daiichi-Sankyo, Takeda Pharmaceutical Co., Biogen Idec Japan, Bayer Yakuhin, Genzyme Japan, Nihon Pharmaceutical Co., and Mitsubishi Tanabe Pharma. Sadako Kuno has served on the advisory board of AbbVie Japan and has received honoraria from Boehringer Ingelheim, GSK, Kyowa Hakko Kirin Co., Novartis, Otsuka Pharmaceutical Co., Dainippon Sumitomo Pharm Co., Ltd., FP Pharmaceutical Co., Ono Pharmaceutical Co., AbbVie Japan, and Alfresa Pharma. Kazuko Hasegawa has received honoraria from Boehringer Ingelheim, GSK, Kyowa Hakko Kirin Co., Novartis, Otsuka Pharmaceutical

doi:10.1002/mdc3.12058

Co., and Dainippon Sumitomo Pharm Co., Ltd. Nobutaka Hattori has worked as a consultant for Hisamitsu Pharmaceutical; has been supported by grants from Otsuka Pharmaceutical, Boehringer Ingelheim, and Kyowa Hakko-Kirin Pharmaceutical Company; and has received honoraria from GSK K.K., Nippon Boehringer Ingelheim, Co., Ltd., FP Pharmaceutical Co., Otsuka Pharmaceutical, Co., Ltd., Dainippon Sumitomo Pharma Co., Ltd., Novartis Pharma K.K., Eisai Co., Ltd., Medtronic, Inc., Kissei Pharmaceutical Company, Janssen Pharmaceutical K.K., Nihon Medi-Physics Co., Ltd., Astellas Pharma Inc., and Kyowa Hakko-Kirin Co., Ltd. Hideki Mochizuki has been supported by grants from Grant-in-Aid for Scientific Research from the Ministry of Education, Culture, Sports, Science and Technology of Japan, Grant-in-Aid for JST-CREST Basic Research Program from the Ministry of Education, Culture, Sports, Science and Technology of Japan, Grant-in-Aid for Scientific Research on Innovative Areas (Brain Environment) from the Ministry of Education, Science, Sports and Culture of Japan, and Grant-in-Aid for Research on Applying Health Technology from the Ministry of Health, Labor and Welfare of Japan; has received honoraria from Biogen Idec Japan, Eisai Co., Ltd., FP Pharmaceutical Co., Elsevier Japan, Hisamitsu Pharma, Kyowa Hakko Kirin Co., GSK, Dainippon Sumitomo Pharm Co., Ltd., FP Pharmaceutical Co., Takeda Pharmaceutical Co., Mitsubishi Tanabe Pharma, Nippon Chemiphar Co., Nihon Medi-Physics Co., Boehringer Ingelheim, Novartis, and UCB Japan; and has received royalties from Nature Japan, Igaku-Shoin, Iyaku Journal, Nanzando Co., and Kinpodo. Hideo Mori has received honoraria from Boehringer Ingelheim, GSK, Otsuka Pharmaceutical Co., Dainippon Sumitomo Pharm Co., Ltd., and FP Pharmaceutical Co. Miho Murata has been supported by grants from the Ministry of Health, Labor and Welfare of Japan and has received honoraria from Boehringer Ingelheim, GSK, Kyowa Hakko Kirin Co., Novartis, Otsuka Pharmaceutical Co., Dainippon Sumitomo Pharm Co., Ltd., and Nihon Medi-Physics Co. Masahiro Nomoto has been awarded grants and research support from the Ministry of Health, Labor and Welfare of Japan, Dainippon Sumitomo Pharm Co., Ltd., Boehringer Ingelheim, Novartis, GSK, FP Pharmaceutical Co., Genzyme, and Tsumura & Co.; has worked as a consultant for and held advisory board membership with honoraria with the Japanese Society of Internal Medicine, Takeda Pharm Co., FP Pharmaceutical Co., Kyowa Hakko Kirin Co., Otsuka Pharm Co., Hisamitsu, Ono Pharm Co., and Meiji Seika; has received honoraria from Boehringer Ingelheim, GSK, Dainippon Sumitomo Pharm Co., Ltd., FP Pharmaceutical Co., Novartis, Kyowa Hakko Kirin Co., Otsuka Pharm Co., Genzyme, Panasonic Healthcare Co., and UCB Inc.; and has received royalties from Maruzen, Igaku-Shoin, and Nishimura. Ryosuke Takahashi has worked as a consultant for KAN Research Institute, Inc., and Daiichi-Sankyo; has been awarded grants and research support from Dainippon Sumitomo Pharm Co., Ltd., Boehringer Ingelheim, Novartis, Pfizer Co., Ltd., GSK, Takeda Pharmaceutical Co., Mitsubishi Tanabe Pharma, and Kyowa Hakko Kirin Co.; and has received honoraria from Boehringer Ingelheim, GSK, Dainippon Sumitomo Pharm Co., Ltd., FP Pharmaceutical Co., Medical Review, Novartis, Daiichi-Sankyo, Kyowa Hakko Kirin Co., Mitsubishi Tanabe Pharma, Eisai Co., Ltd., Nihon Pharmaceutical Co., Otsuka Pharmaceutical Co., Janssen Pharmaceutical Company, Sanofi, Alfresa Pharma Co., Japan Blood Products Organization, Asbio Pharma Co., Ltd., and MSD. Atsushi Takeda has been supported by grants from the Ministry of Education, Culture, Sports, Science and Technology of Japan and the Ministry of Health, Labor and Welfare of Japan; has received honoraria from Otsuka Pharmaceutical Co., Kyowa Hakko Kirin Co., Ltd., GSK, Daiichi-Sankyo, Dainippon Sumitomo Pharm Co., Ltd., FP Pharmaceutical Co., Takeda Pharmaceutical Co., Boehringer Ingelheim, Novartis, and Ono Pharmaceutical; and has received royalties from Iyaku Journal, Chugai-Igakusha, Igaku-Shoin, Medical View, Elsevier Japan, and Aruta Shuppan. Yoshio Tsuboi has been supported by grants from the Ministry of Health, Labor and Welfare of Japan and has received honoraria from Eisai Co., Ltd., Otsuka Pharmaceutical Co., Kyowa Hakko Kirin Co., GSK, Daiichi-Sankyo, Dainippon Sumitomo Pharm Co., Ltd., FP Pharmaceutical Co., Mitsubishi Tanabe Pharma, Teijin Pharma, Boehringer Ingelheim, and Novartis. Yoshikazu Ugawa has been supported by grants from the Ministry of Education, Culture, Sports, Science and Technology of Japan, the Ministry of Health, Labor and Welfare of Japan, the Support Center for Advanced Telecommunications Technology Research, the Association of Radio Industries Businesses, the Uehara Memorial Foundation, Novartis Foundation (Japan) for the Promotion of Science, JST, and Nihon Kohden; has received honoraria from the Taiwan Society of Clinical Neurophysiology, Indonesia Society of Clinical Neurophysiology, Taiwan Movement Disorders Society, Astellas Pharma, Eisai Co. Ltd., Dainippon Sumitomo Pharm Co., Ltd., FP Pharmaceutical Co., Otsuka Pharmaceutical Co., Elsevier Japan, Kissei Pharmaceutical Co., Kyorin Pharma, Kyowa Hakko Kirin Co., GSK, Sanofi, Daiichi-Sankyo, Takeda Pharmaceutical Co., Mitsubishi Tanebe Pharma, Teijin Pharma, Nippon Chemiphar Co., Nihon Pharmaceutical Co., Boehringer Ingelheim, Novartis, Bayer Yakuhin, and Mochida Pharma; and has received royalties from Chugai-Igakusha, Igaku-Shoin Ltd., Medical View, and Blackwell Publishing. Mitsutoshi Yamamoto has received honoraria from Dainippon Sumitomo Pharm Co., Ltd., Boehringer Ingelheim, Novartis, GSK, FP Pharmaceutical Co., Kyowa Hakko Kirin Co., and Otsuka Pharm Co. Fusako Yokochi has received honoraria from GSK, Otsuka Pharmaceutical Co., Medtronic, and AbbVie Japan. Fumihito Yoshii has been supported by grants from Eisai Co., Ltd., Dainippon Sumitomo Pharm Co., Ltd., FP Pharmaceutical Co., Takeda Pharmaceutical Co., Mitsubishi Tanabe Pharma, GSK, Boehringer Ingelheim, Daiichi-Sankyo, Mitsubishi Tanabe Pharma, and Pfizer and has received honoraria from GSK, Dainippon Sumitomo Pharm Co., Ltd., Boehringer Ingelheim, Novartis, AbbVie Japan, Ono Parmaceutical Co., Otsuka Pharmaceutical Co., and Janssen Pharmaceutical Co. Glenn T. Stebbins has worked as a consultant for and held advisory board membership with honoraria with Adamas Pharmaceuticals, Inc., Ceregene, Inc., Child Health and Development Institute (CHDI) Management,

doi:10.1002/mdc3.12058

Inc., Ingenix Pharmaceutical Services (i3 Research), and Neurocrine Biosciences, Inc.; has been awarded grants and research support from the National Institutes of Health (NIH), the Michael J. Fox Foundation (MJFF) for Parkinson's Research, and the Dystonia Coalition; has received honoraria from the International Parkinson and Movement Disorder Society (MDS), American Academy of Neurology, and the MJFF; and has received a salary from Rush University Medical Center. Barbara C. Tilley has been awarded grants from the NIH (National Institute of Neurological Disorders and Stroke, National Heart, Lung and Blood Institute, National Institute on Minority Health and Health Disparities, and National Institute of General Medical Sciences), the Pfizer Data and Safety Monitoring Committee and the NIH Data and Safety Monitoring Committees and has received a salary from the University of Texas Health Science Center School of Public Health at Houston, Division of Biostatistics. Sheng Luo and Lu Wang have nothing to declare. Nancy R. Lapelle has worked in cognitive testing, qualitative research, and program/process evaluation consulting for the UMass Medical School (UMMS) Lamar Soutter Library, UMass Medical School Inter-Professional Development, The Association of Academic Health Sciences Libraries, Medical University of South Carolina (MUSC) College of Nursing and Hollings Cancer Center, and the MDS; Dr. Lapelle is a subcontractor on a variety of research and evaluation grants with principal investigators at UMMS and MUSC. Christopher G. Goetz has worked as a consultant for and held advisory board membership with honoraria with AOP Orphan, Addex Pharma, Advanced Studies of Medicine, Boston Scientific, CHDI, Health Advances, ICON Clinical Research, Inc., Ingenix (i3 Research), the NIH, Neurocrine, Oxford Biomedica, and Synthonics and has been awarded grants and research support with funding from the NIH and the MJFF. Dr. Goetz directs the Rush Parkinson's Disease Research Center that receives support from the Parkinson's Disease Foundation; he directs the translation program for the MDS-UPDRS and UDysRS and receives funds from the MDS for this effort; has received honoraria from the MDS, the American Academy of Neurology, University of Pennsylvania, University of Chicago, and University of Luxembourg; has received royalties from Oxford University Press, Elsevier Publishers, and Wolters Kluwer Health–Lippincott, Wilkins and Williams; and has received a salary from Rush University Medical Center.

APPENDIX The MDS-UPDRS Japanese Validation Study Group

Investigators	Affiliation
Takashi Abe, MD	Department of Neurology, Abe Neurological Clinic
Kenichi Fujimoto, MD	Department of Neurology, Jichi Medical University Hospital
Kazuko Hasegawa, MD	Department of Neurology, National Sagamihara Hospital
Nobutaka Hattori, MD	Department of Neurology, Juntendo University School of Medicine
Yasuto Higashi, MD	Department of Neurology, Himeji Central Hospital
Takaki Imamura, MD	Department of Neurology, Okayama Kyokuto Hospital
Hidehumi Ito, MD	Department of Neurology, Wakayama Medical University
Kazunori Ito, MD	Department of Neurology, Iwamizawa Neurological Medical Clinic
Kenichi Kashihara, MD	Department of Neurology, Okayama Kyokuto Hospital
Jyunya Kawada, MD	Department of Neurology, Shonan Kamakura General Hospital
Noriko Kawashima, MD	Department of Neurology, Kawashima Neurology Clinic
Seiji Kikuchi, MD	National Hospital Organization Hokkaido Medical Center
Sadako Kuno, MD	Kyoto Shijyo Hospital
Tetsuya Maeda, MD	Department of Neurology, Research Institute for Brain and Blood Vessels-Akita
Hideki Mochizuki, MD	Department of Neurology, Osaka University Graduate School of Medicine
Hideo Mori, MD	Department of Neurology, Juntendo University Koshigaya Hospital
Kenya Murata, MD	Department of Neurology, Wakayama Medical University
Miho Murata, MD	Department of Neurology, National Center of Neurology and Psychiatry, Parkinson Disease and Movement Disorder Center
Masahiro Nomoto, MD	Department of Neurology and Clinical Pharmacology, Ehime University Graduate School of Medicine
Yasuyuki Okuma, MD	Juntendo University Shizuoka Hospital
Hidemoto Saiki, MD	Department of Neurology, Kitano Hospital
Hideyuki Sawada, MD	National Hospital Organization Utano Hospital
Ryosuke Takahashi, MD	Department of Neurology, Graduate School of Medicine, Kyoto University
Atsushi Takeda, MD	Department of Neurology, Tohoku University Medical School
Asako Takei, MD	Department of Neurology, Hokuyukai Neurological Hospital
Yasuo Terayama, MD	Department of Neurology, Iwate Medical University
Masahiko Tomiyama, MD	Department of Neurology, Aomori Prefectural Central Hospital
Yoshio Tsuboi, MD	Department of Neurology, Fukuoka University Medical School
Yoshikazu Ugawa, MD	Department of Neurology, Fukushima Medical University
Mitsutoshi Yamamoto, MD	Takamatsu Neurology Clinic
Fusako Yokochi, MD	Department of Neurology, Tokyo Metropolitan Neurological Hospital
Kazuto Yoshida, MD	Department of Neurology, Japanese Red Cross Asahikawa Hospital
Fumihito Yoshii, MD	Department of Neurology, Tokai University School of Medicine

Investigators involved in the cognitive pretesting and/or validation and their affiliations.

doi:10.1002/mdc3.12058

References

1. Fahn S, Elton RL. Unified Parkinson's Disease Rating Scale. In: Fahn S, Marsden CD, Goldstein M, Calne DB, eds. *Recent Developments in Parkinson's Disease*, Vol. 2. Florham Park, NJ: MacMillan Healthcare Information; 1987:153–164.
2. Movement Disorder Society Task Force on Rating Scales for Parkinson's Disease. The Unified Parkinson's Disease Rating Scale (UPDRS): status and recommendations. *Mov Disord* 2003;18: 738–750.
3. Barone P, Antonini A, Colosimo C, et al. The PRIAMO study: a multicenter assessment of nonmotor symptoms and their impact on quality of life in Parkinson's disease. *Mov Disord* 2009;24:1641–1649.
4. Goetz CG, Tilley BC, Shaftman SR, et al. Movement Disorder Society-sponsored revision of the Unified Parkinson's Disease Rating Scale (MDS-UPDRS): scale presentation and clinimetric testing results. *Mov Disord* 2008;23:2129–2170.
5. Antonini A, Abbruzzese G, Ferini-Strambi L, et al. Validation of the Italian version of the Movement Disorder Society-Unified Parkinson's Disease Rating Scale. *Neurol Sci* 2013;34:683–687.
6. Martinez-Martin P, Rodriguez-Blazquez C, Alvarez-Sanchez M, et al. Expanded and independent validation of the Movement Disorder Society-Unified Parkinson's Disease Rating Scale (MDS-UPDRS). *J Neurol* 2013;260:228–236.
7. Fowler FJ. *Improving Survey Questions*. Thousand Oaks, CA: Sage; 1995.
8. Hatcher L. *Step-by-Step Approach to Using the SAS System for Factor Analysis and Structural Equation Modeling*. Cary, NC: SAS Institute; 1994.
9. Muthen LK, Muthen BO. *M-plus User's Guide*. 6th ed. Los Angeles, CA: Muthen & Muthen; 2010.
10. Brown TA. *Confirmatory Factor Analysis for Applied Research*. New York, NY: Guilford SAGE Publications Inc; 2006.
11. Browne MW. An overview of analytic rotation in exploratory factor analysis. *Multivar Behav Res* 2001;36:111–150.
12. Gorsuch RL. *Factor Analysis*. 2nd ed. Hillsdale, NJ: Lawrence Erlbaum Associations Inc; 1983.
13. Forero CG, Maydeu-Olivares A, Gallardo-Pujol D. Factor analysis with ordinal indicators: a Monte Carlo study comparing DWLS and ULS estimation. *Struct Equ Model* 2009;16:625–641.
14. Kimura H, Kurimura M, Wada M, et al. Female preponderance of Parkinson's disease in Japan. *Neuroepidemiology* 2002;21:292–296.
15. Hely MA, Reid WG, Adena MA, et al. The Sydney multicenter study of Parkinson's disease: the inevitability of dementia at 20 years. *Mov Disord* 2008;23:837–844.
16. Morgante L, Colosimo C, Antonini A, et al. Psychosis associated to Parkinson's disease in the early stages: relevance of cognitive decline and depression. *J Neurol Neurosurg Psychiatry* 2012;83:76–82.

doi:10.1002/mdc3.12058

Published January 15, 2015 as 10.3174/ajnr.A4220

Pituitary-Targeted Dynamic Contrast-Enhanced Multisection CT for Detecting MR Imaging–Occult Functional Pituitary Microadenoma

M. Kinoshita, H. Tanaka, H. Arita, Y. Goto, S. Oshino, Y. Watanabe, T. Yoshimine, and Y. Saitoh

ABSTRACT

BACKGROUND AND PURPOSE: Although resection of a tumor by trans-sphenoidal surgery is considered the criterion standard for successful surgical treatment of functional pituitary microadenoma, MR imaging occasionally fails to visualize and identify the tumor and supplementary imaging modalities are necessary. We tested the possibility of dynamic contrast-enhanced multisection CT of the pituitary gland accompanying image reconstruction of contrast agent dynamics to identify the localizations of microadenomas and compared the diagnostic performance with conventional pituitary-targeted MR imaging.

MATERIALS AND METHODS: Twenty-eight patients with surgically confirmed functional pituitary microadenomas (including growth hormone–, adrenocorticotropic hormone–, and prolactin-secreting adenomas) who underwent pituitary-targeted dynamic contrast-enhanced multisection CT were retrospectively investigated. We undertook image reconstruction of the dynamics of the contrast agent around the pituitary gland in a voxelwise manner, visualizing any abnormality and enabling qualification of contrast dynamics within the tumor.

RESULTS: Fifteen cases were correctly diagnosed by MR imaging, while dynamic contrast-enhanced multisection CT correctly diagnosed 26 cases. The accuracy of localization was markedly better for adrenocorticotropic hormone–secreting microadenomas, increasing from 32% on MR imaging to 85% by dynamic contrast-enhanced multisection CT. Compared with the normal pituitary gland, adrenocorticotropic hormone–secreting adenoma showed the least difference in contrast enhancement of the different functional microadenomas. Images acquired at 45–60 seconds after contrast agent injection showed the largest difference in contrast enhancement between an adenoma and the normal pituitary gland.

CONCLUSIONS: Dynamic contrast-enhanced multisection CT combined with image reconstruction of the contrast-enhanced dynamics holds promise in detecting MR imaging–occult pituitary microadenomas.

ABBREVIATIONS: ACTH = adrenocorticotropic hormone; AUC = area under the curve; DCE = dynamic contrast-enhanced; MCT = multisection CT; PRL = prolactin; rAUC = relative AUC

Pituitary microadenoma often shows uncontrolled production of pituitary hormones and causes endocrine disorders such as Cushing disease, acromegaly, and hyperprolactinemia. Although pharmacotherapy has recently played a more pivotal role in treating functional pituitary microadenoma,[1,2] resection of the tumor by trans-sphenoidal surgery is still considered the criterion standard.[3] Because these tumors tend to be relatively small, precise preoperative identification of a microadenoma is one of the crucial elements for successful surgical treatment of this disease.[4]

MR imaging with or without contrast agent is most commonly used for this purpose, and dynamic contrast-enhanced techniques are sometimes applied for better tumor visualization.[5,6] Moreover, the magnetic field strength typically applied in MR imaging has recently increased from 1.5T to 3T, and clearer imaging of microadenomas has thus been anticipated.[4] Such effort, however, often fails to correctly depict the microadenoma, and other modalities such as methionine positron-emission tomography have been suggested to meet this need.[4] Methionine PET does indeed hold promise for the visualization of microadenoma but is not yet widely clinically available, and a more clinically accessible technique is necessary for better visualization of this entity. The present study investigated the possi-

Received September 24, 2014; accepted after revision November 2.

From the Departments of Neurosurgery (M.K., H.A., Y.G., S.O., T.Y., Y.S.) and Radiology (H.T., Y.W.), Osaka University Graduate School of Medicine, Osaka, Japan; Department of Neurosurgery (M.K.), Osaka Medical Center for Cancer and Cardiovascular Diseases, Osaka, Japan; and Department of Neuromodulation and Neurosurgery (Y.S.), Osaka University Graduate School of Medicine, Center of Medical Innovation and Translational Research, Osaka, Japan.

This work was supported by the Aichi Cancer Research Foundation, the SENSHIN Medical Research Foundation, the Life Science Foundation of Japan, and the Japan Society for the Promotion of Science KAKENHI (25462256).

Please address correspondence to Youichi Saitoh, MD, PhD, Department of Neuromodulation and Neurosurgery, Osaka University Graduate School of Medicine, Center of Medical Innovation and Translational Research, 2-2 Yamadaoka, Suita, Osaka 565-0871, Japan; e-mail: neurosaitoh@mbk.nifty.com

Indicates open access to non-subscribers at www.ajnr.org

Indicates article with supplemental on-line tables.

http://dx.doi.org/10.3174/ajnr.A4220

Copyright 2015 by American Society of Neuroradiology.

bility of dynamic contrast-enhanced multisection CT (DCE-MCT) of the pituitary gland accompanying image reconstruction of contrast agent dynamics to identify the location of a microadenoma and compared the diagnostic performance with conventional pituitary-targeted MR imaging.

MATERIALS AND METHODS

Patient Characteristics

The selected patients for this study consisted of a consecutive series of all those with endocrinopathy treated by surgery who had undergone both pituitary-targeted dynamic contrast-enhanced multisection CT and MR imaging as presurgical studies. As a result, pituitary-targeted DCE-MCT was performed for 28 patients with functional pituitary microadenoma at Osaka University Hospital between 2004 and 2014 as a preoperative assessment. Patient characteristics are shown in On-line Table 1. The underlying pathology was adrenocorticotropic hormone (ACTH)-secreting adenoma in 13 cases, growth hormone–secreting adenoma in 6, and prolactin (PRL)-secreting adenoma in 9. The institutional review board of the local ethics committee approved research use of the collected data (institutional review board number: 12491), and written consent was waived for this study.

Preoperative MR Imaging

MR imaging was performed at either 1.5T (Signa Genesis/Excite; GE Healthcare, Milwaukee, Wisconsin; or Magnetom Vision Plus; Siemens, Erlangen, Germany) or 3T (Signa HDxt; GE Healthcare; or Achieva/Ingenia; Philips Healthcare, Best, the Netherlands). Six patients were scanned at 1.5T; and 22, at 3T. Standard T1- and T2-weighted images and gadolinium-enhanced T1-weighted images targeting the pituitary gland were obtained. The dynamic contrast-enhanced technique was not included for MR imaging in the current study. Axial, coronal, and sagittal images were routinely obtained for gadolinium-enhanced T1-weighted imaging. Section thickness was 3 mm, with section spacing ranging from 0.3 to 0.6 mm. Detailed parameters for MR imaging are listed in On-line Table 2. The final diagnostic report from board-certified neuroradiologists was referenced for defining the tumor location. The surgeons (M.K., S.O., Y.S.) and the first author (M.K.) confirmed the radiologists' official report by observing the actual MR imaging.

Preoperative Dynamic Contrast-Enhanced Multisection CT

Pituitary-targeted dynamic contrast-enhanced multisection CT was performed by using either a Discovery CT750 HD, LightSpeed Ultra, or LightSpeed VCT system (GE Healthcare). A schematic presentation of the protocol is provided in Fig 1. One hundred milliliters of 300-mg I/mL contrast agent was injected intravenously with an injection rate of 5 mL/s, and MCT was acquired at 30, 45, 60, and 90 seconds after contrast agent injection. MCT was acquired at 60, 90, 120, and 150 seconds after contrast agent injection for 2 cases and at 40, 80, and 120 seconds for 1 case for technical reasons (On-line Table 1). Approximately 3 seconds were required to acquire each phase in a gapless 3D volume. Subsequently, pituitary-targeted axial images were reconstructed at a special resolution of 0.3/0.3/0.6 mm with no section gap.

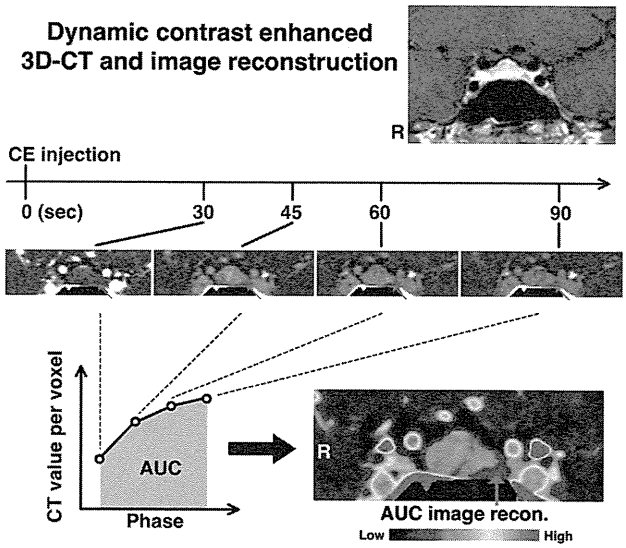

FIG 1. Schematic presentation for DCE-MCT image acquisition and reconstruction. DCE-MCT was performed at 30, 45, 60, and 90 seconds after contrast agent injection. Subsequently, the "AUC image" was reconstructed in 3D. A representative case of a PRL-secreting pituitary microadenoma (case 20) is illustrated. The *red arrows* indicate the microadenoma, which was confirmed by surgical removal of the lesion.

Image Reconstruction of Contrast Agent Dynamics and Statistical Analysis

The dynamics of the contrast agent around the pituitary gland were calculated by summation of the acquired multiphase MCT in a voxelwise manner by using software developed in-house on Matlab (MathWorks, Natick, Massachusetts). An ROI was placed preoperatively at the normal pituitary gland and the suspected adenoma by the first author (M.K.) on the reconstructed area under the curve (AUC) images without referring to MR imaging, followed by calculation of ROI statistics. A paired t test, 2-way analysis of variance, or 1-way ANOVA with a Tukey multiple comparison test was performed by using GraphPad Prism software, Version 5.0 (GraphPad Software, San Diego, California).

Trans-Sphenoidal Surgery and Verification of the Adenoma

Judgment of tumor location was preoperatively performed by using both MR imaging and DCE-MCT with AUC-reconstructed images. When MR imaging and DCE-MCT led to conflicting results, a surgical approach to the tumor was planned so that both sides within the sella turcica could be explored. Endoscope-assisted trans-sphenoidal surgery was performed in all cases by 3 neurosurgeons specializing in pituitary surgery (M.K., S.O., Y.S.). Histologic or endocrinologic confirmation was undertaken to confirm the presence or absence of a hormone-secreting functional adenoma at the surgical location.

RESULTS

Diagnostic Efficacy of MR Imaging and DCE-MCT for Functional Pituitary Microadenoma

Representative cases are shown in Figs 1 and 2. Figure 1 shows a case of PRL-secreting microadenoma. Contrast-enhanced MR imaging failed to identify tumor within the sella turcica, while

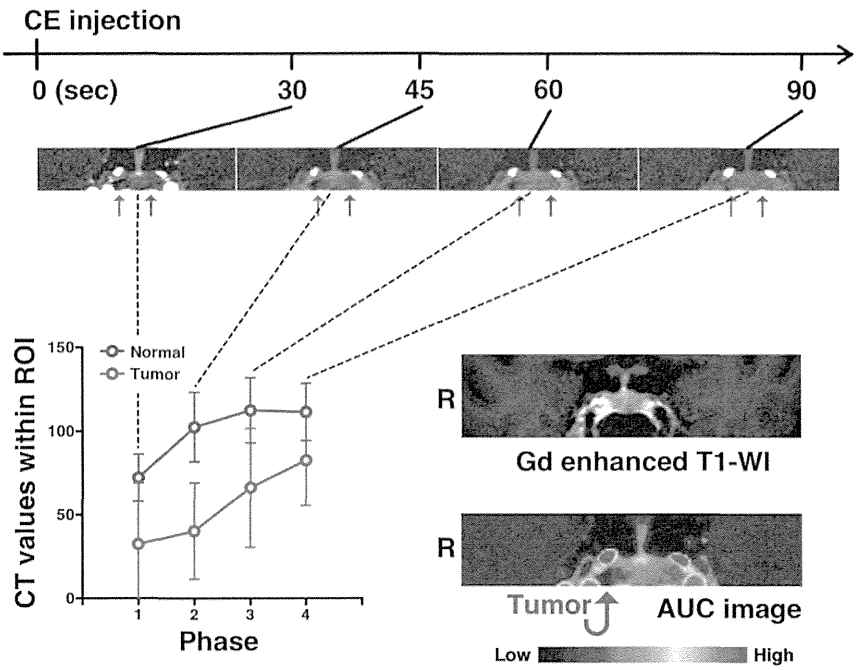

FIG 2. A representative case of ACTH-secreting pituitary microadenoma. DCE-MCT analysis of an ACTH-secreting pituitary microadenoma (case 12) is presented. Abnormal contrast agent dynamics are observed on the right side of the pituitary gland, though no abnormality is evident on MR imaging. The *red arrows* indicate the microadenoma, which was confirmed by surgical removal of the lesion. The *blue arrows* indicate a normal pituitary gland.

Comparison of MRI and CT for correct localization diagnosis of functional microadenomas

Hormone Secreted	No. of Cases	Correct Diagnosis by MRI	Correct Diagnosis by CT
ACTH	13	4	11
GH	6	6	6
PRL	9	5	9
Total	28	15	26

Note:—GH indicates growth hormone.

DCE-MCT clearly showed decreased and delayed contrast enhancement on the left side of the pituitary gland. Abnormal contrast agent dynamics were much more easily appreciated on the reconstructed AUC image. Figure 2 shows a case of ACTH-secreting microadenoma. Contrast-enhanced MR imaging again failed to identify the presence of tumor, while DCE-MCT along with the reconstructed AUC image clearly suggested a lesion located on the right side of the pituitary gland. Diagnostic performances of MR imaging and DCE-MCT for each type of functional pituitary microadenoma are listed in the Table and On-line Table 1. Overall, 15 of the 28 cases were correctly diagnosed by MR imaging, while DCE-MCT correctly diagnosed 26 cases (Table). The accuracy of location prediction was markedly improved for ACTH-secreting microadenoma, increasing from 32% (4/13) with MR imaging to 85% (11/13) with DCE-MCT.

Comparison of Contrast-Enhancement Dynamics between the Normal Pituitary Gland and a Functional Pituitary Microadenoma by DCE-MCT

The dynamics of contrast enhancement were compared between the normal pituitary gland and a functional pituitary microadenoma by looking into differences in the AUC retrieved by DCE-MCT. ROIs were placed on either the normal-appearing pituitary gland or the adenoma, the locations of which were confirmed postoperatively. AUC was significantly decreased in the microadenoma compared with the normal pituitary gland (Fig 3*A*). Relative AUC (rAUC) was subsequently calculated for each lesion, as $rAUC = AUC_{adenoma}/AUC_{pituitary}$. When contrast-enhanced dynamics are equal between the adenoma and the normal pituitary gland, the rAUC will thus be 1. Fig 3*B* shows that ACTH-secreting adenomas presented with a significantly higher rAUC compared with PRL-secreting adenomas, and the rAUC of ACTH-secreting adenoma was close to 1. A trend was also seen for the growth hormone–secreting adenoma to show lower rAUC than the ACTH-secreting adenoma. These results suggest that the contrast-enhanced dynamics of ACTH-secreting microadenomas are relatively similar to those of the normal pituitary gland compared with PRL- or growth hormone–secreting microadenomas. This finding was also confirmed by analyzing the ratio of contrast enhancement compared with the normal pituitary gland in each phase during DCE-MCT. The ACTH-secreting adenoma showed the least contrast-enhancement differences compared with the normal pituitary gland (Fig 3*C*). These differences were significant ($P = .01$, 2-way ANOVA). In addition, the time phase that showed the largest difference in contrast enhancement between the adenoma and the normal pituitary gland was 45–60 seconds after contrast agent injection, irrespective of the secreted hormone.

DISCUSSION

Successful surgical treatment of functional pituitary microadenoma largely relies on accurate identification of the tumor within the sella turcica.[4] These relatively small tumors represent a challenge to both neuroradiologists and neurosurgeons in locating them, resulting in a greater potential for insufficient treatment of the lesion. The criterion standard technique used for lesion localization is MR imaging,[5-7] and some clinical investigations have suggested contrast-enhanced CT,[8,9] super-selective venous sampling of pituitary hormone levels,[10-12] and methionine PET[4] as useful modalities to supplement MR imaging findings. The clinical values of these additional presurgical studies, however, remain undetermined, and conflicting results have been reported. For example, one report has claimed that venous sampling of ACTH at the inferior petrosal sinus is informative for determining adenoma location,[12] while others have reported results to the contrary.[11] Methionine PET has also been proposed as a promising imaging technique to identify MR imaging–occult ACTH-secreting microadenomas. MR imaging–registered methionine PET was previously reported

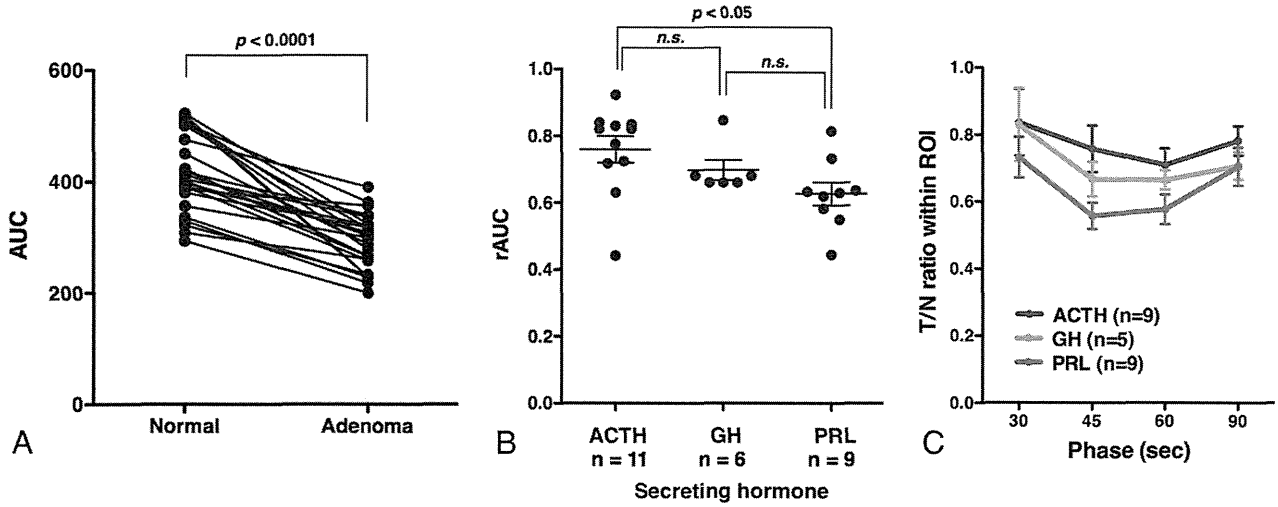

FIG 3. Contrast agent dynamics of pituitary microadenomas assessed by AUC. *A*, Adenomas show significantly lower AUC compared with the normal pituitary gland ($P < .0001$, paired *t* test). *B*, ACTH-secreting pituitary microadenomas show significantly higher rAUC compared with PRL-secreting microadenomas ($P < .05$, 1-way ANOVA with a Tukey multiple comparison), suggesting that contrast agent dynamics within ACTH-secreting microadenomas are similar to those of the normal pituitary gland. GH indicates growth hormone. *C*, The ratio of CT values of adenomas to those of the normal pituitary gland (tumor/node ratio [T/n ratio]) is plotted as a function of the time phase during DCE-MCT. Twenty-three cases in which CT acquisition was performed at 30, 45, 60, and 90 seconds were collected. The most significant drop was observed at 45–60 seconds, irrespective of the secreted hormone. In addition, ACTH-secreting adenomas showed the highest tumor/node ratio among the 3 hormones, indicating the least contrast between the adenoma and normal pituitary gland (2-way ANOVA, $P = .01$).

as showing superb performance in detecting ACTH-secreting microadenomas, of which identification was significantly difficult by using MR imaging alone.[4] The availability of methionine PET, however, remains limited, and more extensive studies are required to confirm the clinical value of methionine PET for diagnosing functional microadenoma.

MR imaging shows several technical limitations in elucidating the presence of microadenoma. The above-mentioned small size of the tumor is one. To guarantee sufficient image quality, we usually select a section thickness of 3 mm for pituitary imaging. Given the sizes of microadenomas, which are <10 mm, there is a high chance of overlooking the lesion. In addition to the problem of size, pituitary adenoma imaging by using a contrast agent largely relies on the adenomas showing much less contrast enhancement than the normal pituitary gland. As Fig 3*B* suggests, an ACTH-secreting microadenoma, in particular, shows contrast-enhanced dynamics similar to that of the normal pituitary gland, which seems likely to contribute to failed detection of the lesion on MR imaging. Although the dynamic contrast-enhanced technique is often applied on MR imaging to overcome this issue, scanning time usually required to obtain each dynamic phase ranges from 20 to 30 seconds[6] or is shortened into 12–20 seconds in some cases, but it is not possible to obtain a gapless 3D image as in MCT. Figure 3*C*, in particular, highlights this problem. The most suitable time phase to obtain sufficient contrast between an adenoma and the normal pituitary gland is 45–60 seconds after contrast agent injection. This adenoma/normal pituitary gland contrast will rapidly diminish within the subsequent 30 seconds. Both spatial and temporal resolution must, therefore, be sufficiently high to visualize the presence of the adenoma.

The proposed CT-based imaging technique has the potential to overcome these technical difficulties associated with MR imaging, mainly due to the superior temporal resolution of CT compared with MR imaging. Each phase of MCT can be acquired in a full 3D image within 3 seconds, which provides satisfactory spatial and temporal resolution. The idea of using DCE-MCT for microadenoma detection has been proposed before.[8,9] To better visualize contrast-enhancement dynamics in a voxelwise manner, the present study applied image reconstruction. The resulting AUC images provided intuitive images for clinicians to identify lesions with abnormal contrast-enhancement dynamics.

Limitations of the current study should be mentioned. First, this study was not a direct comparison between DCE–MR imaging and DCE-MCT. The patient cohort for this study did not have DCE–MR imaging as presurgical imaging for pituitary microadenomas. Further study is necessary to critically evaluate the clinical value of DCE-MCT with an image-reconstruction technique compared with conventional DCE–MR imaging. Another concern is the MR image quality of the current study. Previous studies reported exhibiting 66%–100% sensitivity in detecting ACTH-secreting microadenoma[6,7] with the aid of DCE–MR imaging. The sensitivity of the current study for detecting ACTH-secreting microadenomas was as low as 32%, which may suggest that MR images of the current study might have been suboptimized compared with the past literature reports. In addition, although it is intriguing to contemplate why ACTH-secreting microadenomas show different contrast-enhanced dynamics compared with other functional microadenomas as shown in Fig 3*C*, the pathology of the blood supply to microadenomas is unfortunately not yet well-understood, making it difficult to reach any conclusive argument on this matter.

In summary, the present results show that DCE-MCT images along with AUC images can help identify microadenomas and improve the overall detection of those lesions compared with MR imaging alone. Although this study was not a direct comparison between DCE–MR imaging and DCE-MCT, it seems valid to conclude that DCE-MCT is a noninvasive diagnostic technique, which, along with the reported AUC reconstruction method,

could be recommended as a supplementary diagnostic technique for MR imaging–occult functional microadenoma.

CONCLUSIONS

Dynamic contrast-enhanced multisection CT combined with image reconstruction of the contrast-enhanced dynamics holds promise in detecting MR imaging–occult pituitary microadenoma. Because surgical outcomes are highly reliant on accurate preoperative identification of the adenoma, the proposed technique should contribute to better surgical outcomes for functional pituitary microadenomas.

Disclosures: Manabu Kinoshita—*RELATED: Grant*: Research Grant from the Life Science Foundation of Japan,* Scientific Research (C) from the Japan Society for the Promotion of Science,* Research Grant from the SENSHIN Medical Research Foundation,* Research Grant from the Aichi Cancer Research Foundation*; *UNRELATED: Grants/Grants Pending*: Research Grant from the Japanese Foundation for Multidisciplinary Treatment of Cancer.* Yoshiyuki Watanabe—*UNRELATED: Grants/Grants Pending*: Toshiba Medical Japan,* *Comments*: research fund about 320-row CT; *Payment for Lectures (including service on Speakers Bureaus)*: GE Healthcare, Bayer Pharmaceutical. Youichi Saitoh—*UNRELATED: Consultancy*: Teijin Pharma; *Payment for Lectures (including service on Speakers Bureaus)*: Teijin Pharma. *Money paid to the institution.

REFERENCES

1. Colao A, Boscaro M, Ferone D, et al. **Managing Cushing's disease: the state of the art.** *Endocrine* 2014;47:9–20
2. Suda K, Inoshita N, Iguchi G, et al. **Efficacy of combined octreotide and cabergoline treatment in patients with acromegaly: a retrospective clinical study and review of the literature.** *Endocr J* 2013; 60:507–15
3. Starke RM, Raper DM, Payne SC, et al. **Endoscopic vs microsurgical transsphenoidal surgery for acromegaly: outcomes in a concurrent series of patients using modern criteria for remission.** *J Clin Endocrinol Metab* 2013;98:3190–98
4. Ikeda H, Abe T, Watanabe K. **Usefulness of composite methionine–positron emission tomography/3.0-Tesla magnetic resonance imaging to detect the localization and extent of early-stage Cushing adenoma.** *J Neurosurg* 2010;112:750–55
5. Lee HB, Kim ST, Kim HJ, et al. **Usefulness of the dynamic gadolinium-enhanced magnetic resonance imaging with simultaneous acquisition of coronal and sagittal planes for detection of pituitary microadenomas.** *Eur Radiol* 2012;22:514–18
6. Portocarrero-Ortiz L, Bonifacio-Delgadillo D, Sotomayor-González A, et al. **A modified protocol using half-dose gadolinium in dynamic 3-Tesla magnetic resonance imaging for detection of ACTH-secreting pituitary tumors.** *Pituitary* 2010;13:230–35
7. Kasaliwal R, Sankhe SS, Lila AR, et al. **Volume interpolated 3D-spoiled gradient echo sequence is better than dynamic contrast spin echo sequence for MRI detection of corticotropin secreting pituitary microadenomas.** *Clin Endocrinol* 2013;78:825–30
8. Abe T, Izumiyama H, Fujisawa I. **Evaluation of pituitary adenomas by multidirectional multislice dynamic CT.** *Acta Radiol* 2002;43: 556–59
9. Bonneville JF, Cattin F, Gorczyca W, et al. **Pituitary microadenomas: early enhancement with dynamic CT–implications of arterial blood supply and potential importance.** *Radiology* 1993;187:857–61
10. Batista D, Gennari M, Riar J, et al. **An assessment of petrosal sinus sampling for localization of pituitary microadenomas in children with Cushing disease.** *J Clin Endocrinol Metab* 2006;91: 221–24
11. Lefournier V, Martinie M, Vasdev A, et al. **Accuracy of bilateral inferior petrosal or cavernous sinuses sampling in predicting the lateralization of Cushing's disease pituitary microadenoma: influence of catheter position and anatomy of venous drainage.** *J Clin Endocrinol Metab* 2003;88:196–203
12. Teramoto A, Yoshida Y, Sanno N, et al. **Cavernous sinus sampling in patients with adrenocorticotrophic hormone–dependent Cushing's syndrome with emphasis on inter- and intracavernous adrenocorticotrophic hormone gradients.** *J Neurosurg* 1998;89:762–68

Jpn J Rehabil Med 2014 ; **51** : 645–649

《教育講演》

神経リハビリテーションにおける近赤外分光法の応用*1

三原 雅史*2

Functional Near Infrared Spectroscopy in Neurorehabilitation*1

Masahito MIHARA*2

Abstract : Functional Near-Infrared Spectroscopy (fNIRS) is a characteristically functional neuroimaging technique which enables us to measure the daily tasks related to cortical activation including gait and postural task. Using fNIRS, it was found that the medial sensorimotor and supplementary motor area play an important role in gait and postural control in healthy subjects. In addition, it was also revealed that the individual balance ability was correlated with the cortical activation in the supplementary motor area during the postural task. These findings supported the notion that the supplementary motor area is one of the key structures for balance recovery in stroke patients. Not only can fNIRS effectively monitor the functional reorganization of the central nervous system, but fNIRS has also been used as a therapeutic tool. With recent advances in technique enabling real-time decoding of brain activity, functional neuroimaging can now be used as a neurofeedback tool, in which the voluntary modulation of cortical activation is available. After we developed a working fNIRS mediated neurofeedback system and confirmed its neuromodulation effect in healthy subjects, we investigated its clinical efficacy as a therapeutic tool for augmenting the functional recovery after stroke. Our pilot randomized control study revealed the promising result that neurofeedback intervention could improve finger function in chronic stroke patients including patients with moderate to severe paresis. These findings provide a new therapeutic possibility for those patients who gain only limited functional recovery from conventional rehabilitative interventions in the chronic stage. (**Jpn J Rehabil Med 2014 ; 51 : 645–649**)

Key words : 脳卒中 (stroke), 神経可塑性 (neuroplasticity), 近赤外分光法 (near infrared spectroscopy), ニューロフィードバック (neurofeedback)

はじめに

近年の脳機能画像技術の発展によって，ヒトにおける様々な神経活動が非侵襲的に測定できるようになってきている．様々な脳機能画像技術の中でも，磁気共鳴画像 (magnetic resonance imaging：MRI) 装置を用いた機能的 MRI (functional MRI：fMRI) は最も多くの研究者によって用いられており，これまでに様々な神経科学的知見をもたらしている．しかしながら，MRI 装置の特性上，fMRI での脳活動測定は通常安静臥位で施行可能な課題に限られ，リハビリテーション (以下，リハ) 分野における応用には制限もあった．本稿で紹介する機能的近赤外分光法 (functional Near Infrared Spectroscopy：fNIRS) は fMRI 同様に神経活動に伴う局所脳血流変化を測定する技術であり，立位や座位などより日常生活動作に近い課題での脳活動が測定可能というメリットがあり，リハの分野での応用において有利であると考える．本稿では，fNIRS を用いたリハ分野での応用について，これまでの知見と将来的な展望を含めて紹介する．

2014 年 1 月 6 日受稿

*1 本稿は第 8 回日本リハビリテーション医学会専門医会学術集会教育講演 (2013 年 11 月 10 日，札幌) をまとめたものである．

*2 大阪大学大学院医学系研究科神経内科学/〒 565–0871 大阪府吹田市山田丘 2–2　D4
Department of Neurology, Osaka University Graduate School of Medicine
E-mail : mihara@neurol.med.osaka-u.ac.jp

近赤外分光法について

特定の波長帯（650～900 nm）における近赤外光は皮膚や骨に対して高い透過性を有する一方，ヘモグロビンやミオグロビンなどの生体内色素によって吸収されるという特徴を有している．fNIRSはこの近赤外光の特徴を利用して，頭皮上から非侵襲的に大脳皮質における局所血流変化を測定する技術である[1,2]．ある波長の光が照射されたときの吸光度が試料中における吸光物質濃度と通過距離（光路長）の積に比例するというmodified Beer-Lambert則を用いて，課題中の酸素化および脱酸素化ヘモグロビンの濃度変化を測定し，複数の部位での測定を同時に行うことで，機能的脳画像として大脳皮質活動をトポグラフィー表示することが可能である．

fNIRSの特徴として，頭皮と照射/検出ファイバーとの密着が確保されていれば，測定中の姿勢や体位に関する制限が少なく，ベッドサイドなどの日常生活環境場面での測定が可能であるという利点がある一方で，原理上，近赤外光が到達しにくい脳深部の活動測定は困難であり，空間分解能は1～数cm程度に留まるという欠点もある．これらの特徴を活かして，我々は，fNIRSを用いた立位歩行障害に関わる神経機能の解明に取り組んでいる．

立位歩行中の大脳皮質活動

これまでの動物実験の結果から，姿勢や歩行は脊髄，脳幹・小脳などを含む多くの中枢神経領域による階層的支配によって調整されていることが明らかになっている[3~6]．さらに，ヒトにおける二足立位歩行

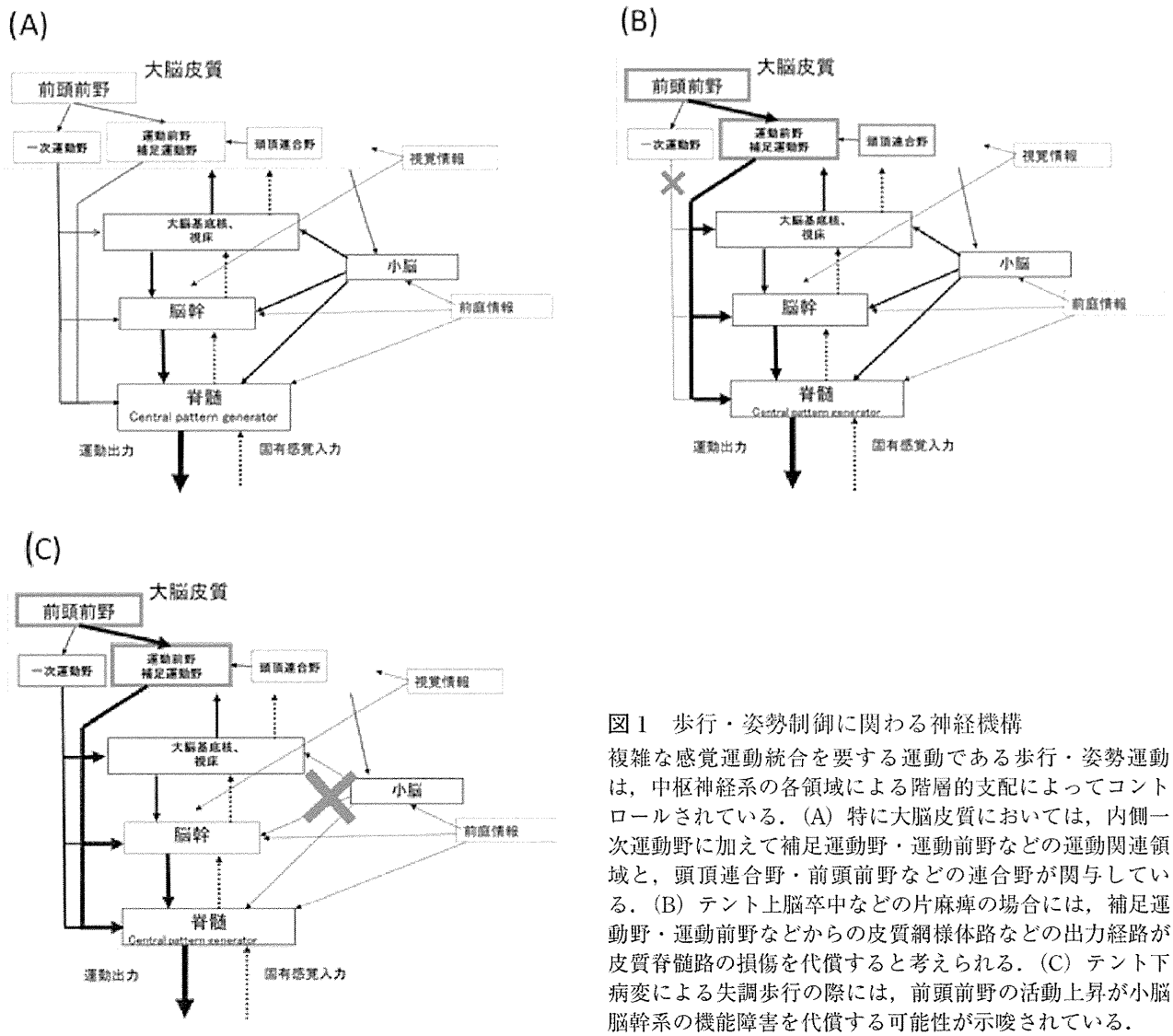

図1　歩行・姿勢制御に関わる神経機構
複雑な感覚運動統合を要する運動である歩行・姿勢運動は，中枢神経系の各領域による階層的支配によってコントロールされている．(A) 特に大脳皮質においては，内側一次運動野に加えて補足運動野・運動前野などの運動関連領域と，頭頂連合野・前頭前野などの連合野が関与している．(B) テント上脳卒中などの片麻痺の場合には，補足運動野・運動前野などからの皮質網様体路などの出力経路が皮質脊髄路の損傷を代償すると考えられる．(C) テント下病変による失調歩行の際には，前頭前野の活動上昇が小脳脳幹系の機能障害を代償する可能性が示唆されている．

は潜在的に不安定であり，ヒトにおいて高度に発達した大脳皮質の関与が更に大きいことが推測される．我々は，fNIRSを用いた検討によって，立位歩行調節における大脳皮質の関与について検討を行った．

fNIRSを用いた健常者における起立歩行中の大脳皮質活動としては，トレッドミル歩行課題を用いた検討で，内側一時運動野や細く運動野などの関与が報告されている[7]．また，歩行速度の変化など環境に対する歩行速度の調整や歩行の構え・準備などの際には前頭前野の活動が関与することも報告されている[8]．立位姿勢保持に関しては，外乱を加えた際の立位姿勢維持には前頭前野の関与が示唆されており，特に意図的な姿勢の維持には補足運動野や頭頂連合野の関与が大きいことが示唆されている[9]（図1）．

さらに，脳卒中患者における立位歩行中の脳活動変化についての検討を行った．テント上病変に伴う片麻痺を呈する患者では，歩行能力の改善にともなって対側一次運動野・および両側の運動前野・前頭前野などの活動上昇が認められている[10,11]．一方で，テント下病変に伴う失調歩行患者においては，健常者において歩行開始時にのみ認める前頭前野活動が定常歩行中にも遷延して認められ，小脳との強い機能的結合を有する前頭前野が脳幹小脳系の障害に伴う失調性歩行障害を代償している可能性が考えられた[12]．

脳卒中後片麻痺患者における立位姿勢保持の際の大脳皮質活動の検討では，横断的検討において患者の臨床的なバランス評価とバランス課題中の両側補足運動野の活動の間に相関を認め（図2）[13]，縦断的検討においても集中リハによるバランス能力の改善と介入前後でのバランス課題中の補足運動野の活動変化との間に有意な相関が認められるなど[14]，脳卒中後のバランス能力改善に補足運動野が深く関与している可能性が示唆された．

新しい治療介入手段としてのfNIRS

リハ分野におけるfNIRSの応用は，これまで，主に上述のような脳損傷後の機能的再構成のモニタリングによる予後予測や治療効果判定を目的とした測定機器としての利用が多かった．しかしながら，近年脳情報を測定・解読して機器制御を行うBrain-Machine Interface（BMI）など脳情報解読技術の進歩により，脳機能画像を用いた治療介入の試みがなされるようになってきている．特に，脳情報をリアルタイムに解読し，その活動を被験者に提示することで随意的に脳活動の制御を行うNeurofeedbackは，外的な刺激を用いることなく脳機能に対する介入を可能とするNeuro-

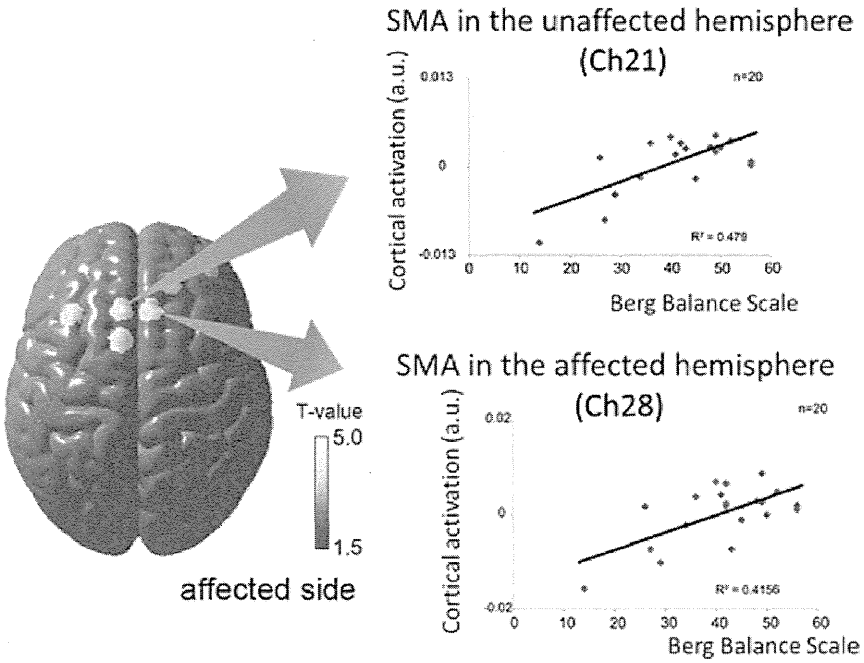

図2　脳卒中後のバランス能力と，脳活動との関係
脳卒中後片麻痺患者におけるバランス課題中の脳活動と，各患者のバランス能力との相関．両側補足運動野を中心に，病変側前頭前野，非病変側前頭前野などの領域の活動とバランス能力との間に有意な相関を認める．

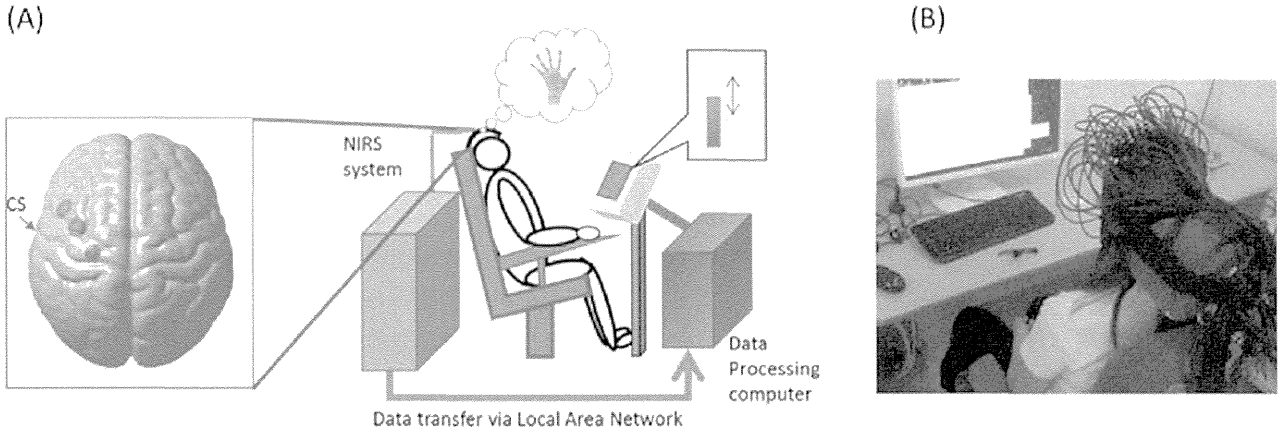

図3　fNIRSを用いたNeurofeedbackシステム

(A) fNIRSを用いて特定の脳領域の活動を計測し，リアルタイムに解析して被験者に提示することで，脳活動を随意的に賦活/抑制する方法を学習する．(B) 実際のNeurofeedback介入の様子．

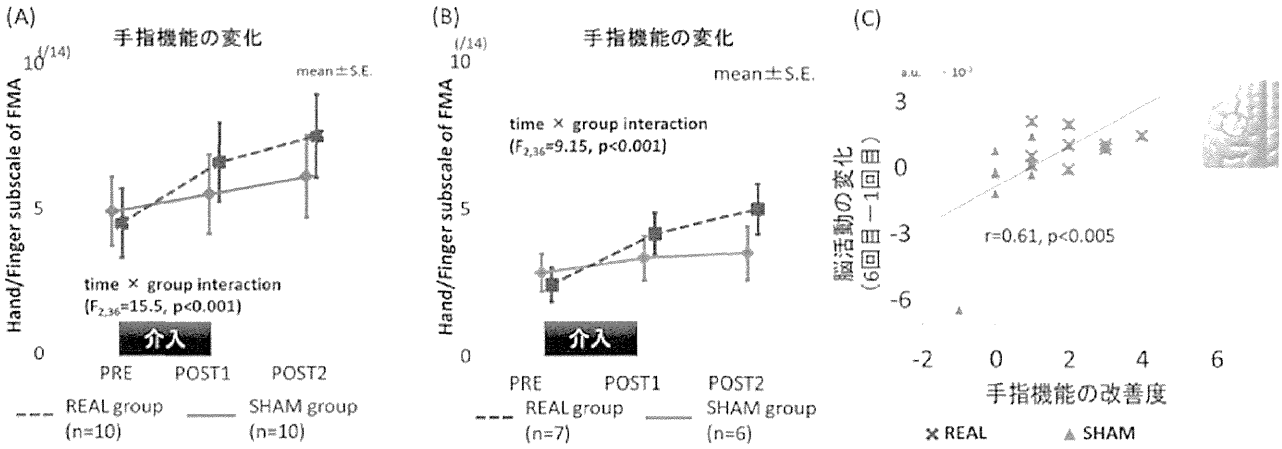

図4　fNIRSを用いたNeurofeedbackによる脳卒中後上肢麻痺に対する効果

(A) 運動想像を用いたNeurofeedbackによって，上肢機能の改善効果が促進された．(B) Fugl-Meyer手指スケールが4点以下の重症群においても，Neurofeedbackの効果が認められた．(C) 運動想像中の病変側運動前野の活動変化と手指機能の改善度との間に有意な相関関係が認められた．

modulation技術の1つで，以前から脳波を用いたシステムはADHD治療などの分野で用いられてきている[15]．fMRIを用いたNeurofeedbackシステムでも視覚機能の改善[16]や疼痛治療などへの応用[17]が進められている．

fMRIを用いたシステムは空間解像度が高く，先行研究によって蓄積された知見を用いることができる利点があるものの，装置の規模が大きく，介入中の体動が制限されるなど，臨床現場での治療介入においては不利な点もあった．これらの点を改善するために，我々は，臨床場面での有用性向上を目指して，患者への負担が少ないfNIRSを応用したNeurofeedbackシステムを開発し[18]，健常者での運動想像中の対側運動関連領域をターゲットとしたNeurofeedbackが，運動想像中の運動前野活動を賦活し，運動感覚的な運動想像を誘導することを明らかにした（図3）．

運動想像，特に自分自身の体が動いている感覚を伴う運動感覚的な運動想像は，実際の運動と同様の神経基盤を有しており，運動想像を用いた介入が脳卒中患者においても機能改善効果をもたらすことが報告されているが[19]，運動想像を用いた介入はモニターが難しく，その能力にも個人差があるため，介入効果が一定しないという問題点があった．そこで我々は，この運動想像を用いた介入とNeurofeedbackを組み合わせ

ることで，より効率的な介入が可能かどうかを検討した[20]．発症後90日以上経過した上肢麻痺を有する皮質下脳卒中患者20名を対象とし，患者を2群に分けて一方には運動想像中の対側運動前野活動をfeedbackし，もう一方には脳活動とは無関係のランダムな信号をfeedbackし，週3回×2週間，計6回の介入を行って，介入前，介入直後，介入後2週間での麻痺側上肢機能を評価した．実際の脳活動を用いたNeurofeedbackを併用した群（REAL群）では，もう一方の群（SHAM群）と比較して手指機能の改善を認め，重症患者においても有意な効果が認められた．また，Neurofeedback介入による運動想像中の病変側運動前野活動の賦活と手指機能改善度との間に有意な相関関係を認め，Neurofeedbackによる運動前野賦活が機能改善をもたらした可能性が示唆された（図4）．

我々は，これらの結果をもとに，上肢麻痺以外の脳卒中に伴う様々な症状に対する効果や脳卒中以外の疾患に対する有効性を検討中であり，今後，さらに安全で簡便な補助的リハとしてのNeurofeedbackの有用性を高めていきたいと考えている．

おわりに

fNIRSは非侵襲で，簡便な脳機能画像装置として，神経リハ臨床における有用性が高い．日常生活場面での測定が可能で，被験者に対する制約が少ないというfNIRSの特徴を生かすことで，従来の方法では測定が難しかった，脳損傷後の立位歩行に関わる神経ネットワークの経時的変化を捉えることが可能となった．また，測定機器としてだけではなく，Neurofeedbackシステムの一部として，安全で簡便な治療装置としての研究も進んでおり，今後ヘルスケアレベルを含めた幅広い臨床場面での利用も期待される．

文　献

1) Jobsis FF : Noninvasive, infrared monitoring of cerebral and myocardial oxygen sufficiency and circulatory parameters. Science 1977 ; 198 : 1264–1267
2) Cope M, Delpy DT, Reynolds EO, Wray S, Wyatt J, van der Zee P : Methods of quantitating cerebral near infrared spectroscopy data. Adv Exp Med Biol 1988 ; 222 : 183–189
3) Mori S, Iwakiri H, Homma Y, Yokoyama T, Matsuyama K : Neuroanatomical and neurophysiological bases of postural control. Adv Neurol 1995 ; 67 : 289–303
4) Drew T, Prentice S, Schepens B : Cortical and brainstem control of locomotion. Progress in brain research 2004 ; 143 : 251–261
5) Matsuyama K, Mori F, Nakajima K, Drew T, Aoki M, Mori S : Locomotor role of the corticoreticular-reticulospinal-spinal interneuronal system. Progress in brain research 2004 ; 143 : 239–249
6) Mori S, Nakajima K, Mori F, Matsuyama K : Integration of multiple motor segments for the elaboration of locomotion : role of the fastigial nucleus of the cerebellum. Progress in brain research 2004 ; 143 : 341–351
7) Miyai I, Tanabe HC, Sase I, et al : Cortical mapping of gait in humans : a near-infrared spectroscopic topography study. Neuroimage 2001 ; 14 : 1186–1192
8) Suzuki M, Miyai I, Ono T, et al : Prefrontal and premotor cortices are involved in adapting walking and running speed on the treadmill : an optical imaging study. Neuroimage 2004 ; 23 : 1020–1026
9) Mihara M, Miyai I, Hatakenaka M, Kubota K, Sakoda S : Role of the prefrontal cortex in human balance control. Neuroimage 2008 ; 43 : 329–336
10) Miyai I, Yagura H, Oda I, et al : Premotor cortex is involved in restoration of gait in stroke. Ann Neurol 2002 ; 52 : 188–194
11) Miyai I, Yagura H, Hatakenaka M, Oda I, Konishi I, Kubota K : Longitudinal optical imaging study for locomotor recovery after stroke. Stroke 2003 ; 34 : 2866– 2870
12) Mihara M, Miyai I, Hatakenaka M, Kubota K, Sakoda S : Sustained prefrontal activation during ataxic gait : a compensatory mechanism for ataxic stroke ? Neuroimage 2007 ; 37 : 1338–1345
13) Mihara M, Miyai I, Hattori N, et al : Cortical control of postural balance in patients with hemiplegic stroke. Neuroreport 2012 ; 23 : 314–319
14) Fujimoto H, Mihara M, Hattori N, et al : Cortical changes underlying balance recovery in patients with hemiplegic stroke. Neuroimage 2014 ; 85 Pt 1 : 547–554
15) Fuchs T, Birbaumer N, Lutzenberger W, Gruzelier JH, Kaiser J : Neurofeedback treatment for attention-deficit/hyperactivity disorder in children : a comparison with methylphenidate. Appl Psychophysiol Biofeedback 2003 ; 28 : 1–12
16) Shibata K, Watanabe T, Sasaki Y, Kawato M : Perceptual learning incepted by decoded fMRI neurofeedback without stimulus presentation. Science 2011 ; 334 : 1413–1415
17) deCharms RC, Maeda F, Glover GH, et al : Control over brain activation and pain learned by using real-time functional MRI. Proc Natl Acad Sci U S A 2005 ; 102 : 18626–18631
18) Mihara M, Miyai I, Hattori N, et al : Neurofeedback using real-time near-infrared spectroscopy enhances motor imagery related cortical activation. PLoS One 2012 ; 7 : e 32234
19) Page SJ, Levine P, Leonard A : Mental practice in chronic stroke : results of a randomized, placebo-controlled trial. Stroke 2007 ; 38 : 1293–1297
20) Mihara M, Hattori N, Hatakenaka M, et al : Near-infrared spectroscopy-mediated neurofeedback enhances efficacy of motor imagery-based training in poststroke victims : a pilot study. Stroke 2013 ; 44 : 1091–1098